

# Stochastic behaviour in the edge region of the SINP tokamak

Ramesh Narayanan, Md. Nurujjaman and A.N. Sekar Iyengar

Recently, there has been a great deal of importance associated with the effects of magnetic field ergodization in the dynamics of fusion grade plasmas. It is believed that ergodization of the edge magnetic fields can effectively mitigate ELMs and thus improve the confinement properties. The role of the edge electric fields has also generated a lot of interest.

We have carried an experimental scan of the applied vertical magnetic field ( $B_v$ ) in the S.I.N.P. tokamak, wherein an improved confinement regime has been observed. The analysis of the edge region of this set of discharges have been carried out using a Langmuir probe. Nonlinear analysis tools have been invoked to study the possibility of stochastization in the edge plasma signals. We present the results of the above experiments and analysis in this paper.

PACS numbers: 52.25.Gj, 52.25.Xz, 52.55.Fa, 52.70.La, 05.45. -a, 05.45. TP

## I. INTRODUCTION

In fact, a concept of inducing ergodicity in edge magnetic configurations to overcome problems related to plasma-wall interactions has been put forth [6, 7]. A lot of experimental activities have subsequently been carried out in order to implement this concept. In most experiments this stochastic layer is induced externally [8, 9]. However, a stochastic layer can also be inherently present as in W7-X [10, 11]. This has resulted in the emergence of various new applications ranging from the concept of ergodic divertor to the control of transient edge phenomena like ELMs. The stochastization of the peripheral magnetic fields have been experimentally shown to control the plasma dynamics in tokamaks [12].

A new regime was observed in the SINP tokamak wherein the discharge is seen to have a constant current duration, for about 1 ms, after the current dropped down to about half its peak value. This extended duration showed characteristics of improved confinement and was observed to be accompanied by enhanced levels of HX bursts. In order to show the existence of multicascading processes at the edge [13] and to understand the sort of cascading processes we have used the power spectrum, Rescaled (R/S) Range analysis [14] and multifractal analysis.

Section II states briefly about the S.I.N.P. tokamak. Section III presents the experimental results and Section IV the nonlinear analysis methods invoked and the analysis results. Section V discusses the results in this paper.

## II. S.I.N.P. TOKAMAK

The SINP Tokamak ( $R_0 = 30$  cm,  $a = 7.5$  cm) is a small iron core machine having a circular cross-section with two poloidal limiters separated  $180^\circ$  apart from each other [19]. It has an Aluminium conducting shell ( $R_0 = 30$  cm,  $a = 10.9$  cm and thickness = 0.7 cm), comprising of eight sections, made up of four cuts in the toroidal direction and two in the poloidal direction respectively. The penetration time of the conducting shell

is 13 ms without cuts, but due to the presence of the cuts, it is almost instantaneous, ( $\sim 100$   $\mu$ s). The S.I.N.P. tokamak has no plasma position feedback control but we have a vertical magnetic field coil, with the power produced by discharging capacitor banks. Discharges, produced through the Joule Heating (JH) mechanism, can operate in the range of a few kA peak current to a maximum of 75 kA with pulse durations varying from 2 – 5 ms. The toroidal magnetic field ( $B_T$ ) at the minor axis can also be varied upto a maximum of 2 T.

The edge plasma fluctuations are measured using a set of Langmuir and magnetic probes. During the experiments, of data presented in this paper, we have used two Internal Langmuir-Magnetic probe (ILMP) systems which can simultaneously measure the floating potential and poloidal magnetic signals at a given radial location on a shot-to-shot basis. For the purpose of this work, we have analyzed signals from electrostatic probes, mounted in the bottom port of the toroidal chamber, at  $r = 7.5$  cm, i.e. at the radial location containing the inner edge of the poloidal limiter, but toroidally separated by  $21^\circ$  from the latter.

## III. EXPERIMENTAL RESULTS

For the present set of experiments, we kept all parameters like  $B_T = 0.8$  T,  $E_T = 30.6$  V/m, filling pressure, ( $p_{fill}$ ) =  $0.2 \pm 0.05$  mTorr and  $a = 7.5$  cm constant and varied  $B_v$  from a higher value of 54 mT to 6.75 mT. It is observed that discharge duration increases with decrease in  $B_v$  as shown in Figs 1(a), (e) and (i). It is observed that the discharge duration and peak currents are respectively 1.7 ms and 35 kA, at  $B_v = 54$  mT; 2.5 ms and 25.16 kA at  $B_v = 20.25$  mT; 4.5ms and 18 kA at  $B_v = 6.75$  mT. An interesting feature has been observed in Fig 1 wherein the discharge is seen to extend in plasma current duration, after an initial fall to about half its peak value and subsequently remains approximately constant for about 1.5 ms. The instant at which the current extension is observed to begin is denoted as point B [Fig 1]. The extension of the discharge is observed to be accompanied by enhanced hard X-ray (HX) bursts

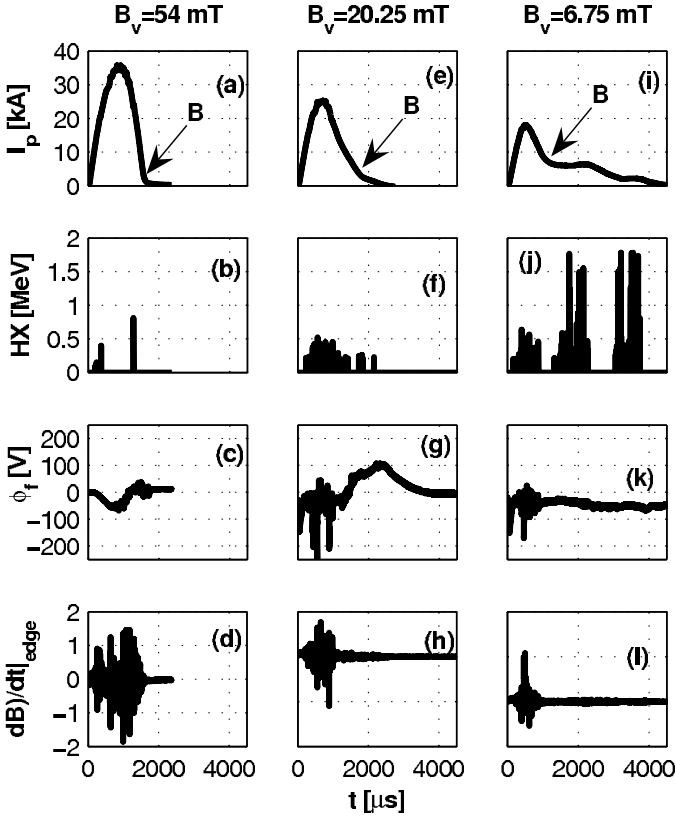


FIG. 1: The depiction of (a),(e),(i) discharge current ( $I_p$ ) evolution; (b),(f),(j)  $3''$  by  $3''$  NaI(Tl) limiter bremsstrahlung bursts; (c),(g),(k) electrostatic probe floating potential ( $\phi_f$ ) signals; & (d),(h),(l) magnetic fluctuation signals for (a)-(d)  $B_v = 54 \text{ mT}$ , (e)-(h)  $B_v = 20.25 \text{ mT}$  and (i)-(l)  $B_v = 6.75 \text{ mT}$

[Fig 1(j)] which is indicative of loss of highly energetic particles from the edge. The electrostatic [Fig. 1(k)] and magnetic fluctuation [Fig. 1(l)] levels are also observed to be reduced during the current extension.

We have analyzed the fluctuations of the extended phase of discharge i.e. after pt B in the range of  $B_v = 13.5 - 20 \text{ mT}$ , using multifractal analysis and time series analysis techniques. We have consider only 512 stationary pt for analysis purpose. For comparison we also have analyzed 512 points(pt) before B. The problem of short data length has been overcome by appending the data to itself to make the length to be 8192 pt for both the cases.

#### IV. ANALYSIS FOR STOCHASTICITY

Linear statistical analysis has been summarized in Fig. 2. Fig. 2(d) shows that the skewness and kurtosis of the signal after the pt B is around 0 and 3 at lower  $B_v$  which indicates the dataset has a normal distribution. For the signal before B it deviates from normal distribution [Fig. 2(c)]. Similar deviation is seen for signals after pt B at higher  $B_v$ .

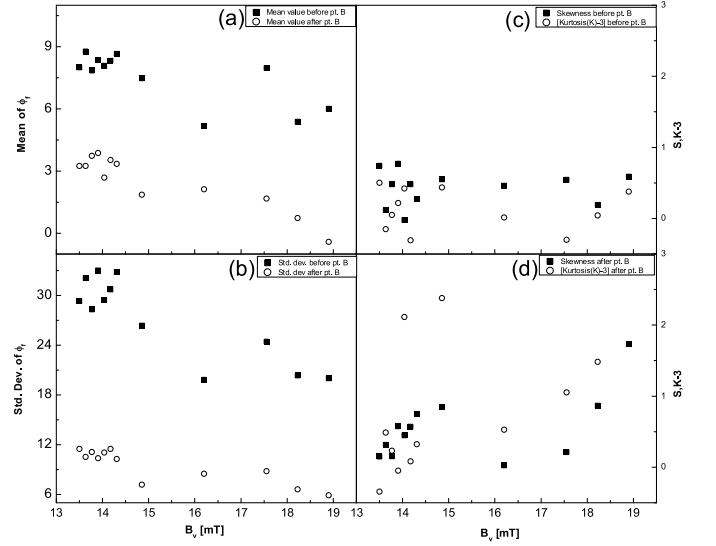


FIG. 2: Estimated statistics of 512 data pts before and after pt. B for various values of  $B_v$ : wherein each subplot depicts (a) mean: before [black, solid square] and after [red, open circle] pt. B, (b) standard deviation: before [black, solid square] and after [red, open circle] pt. B (c) before pt. B: skewness [black, solid square] and kurtosis [red, open circle] (d) after pt. B: skewness [black, solid square] and kurtosis [red, open circle]

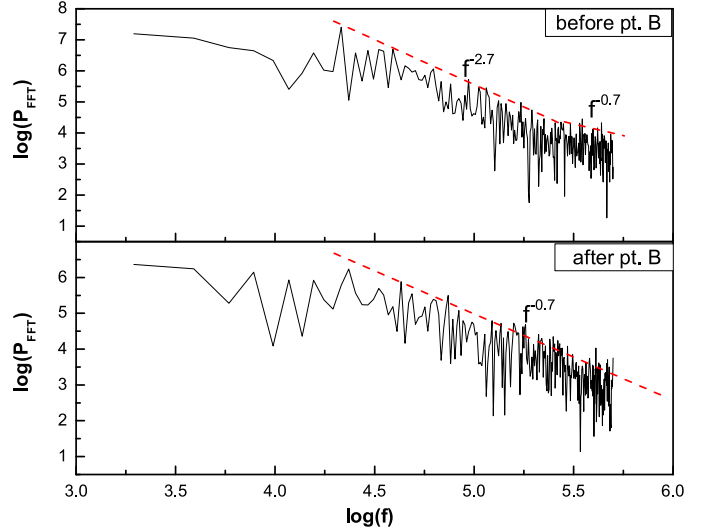


FIG. 3: (color online) Estimated FFT power spectrum, in logarithmic scale, for 512 data pts (a) before pt. B, (b) after pt. B

Hence the edge electrostatic fluctuations in the extended discharge seem to depict stochastic behavior. We, therefore present a detailed analysis of these above signals using techniques like FFT, wavelet analysis, singularity spectrum.

We analyzed the electrostatic fluctuations using the spectral analysis techniques such as the Fast Fourier Transform (FFT) and Wavelet Transforms (WT). The

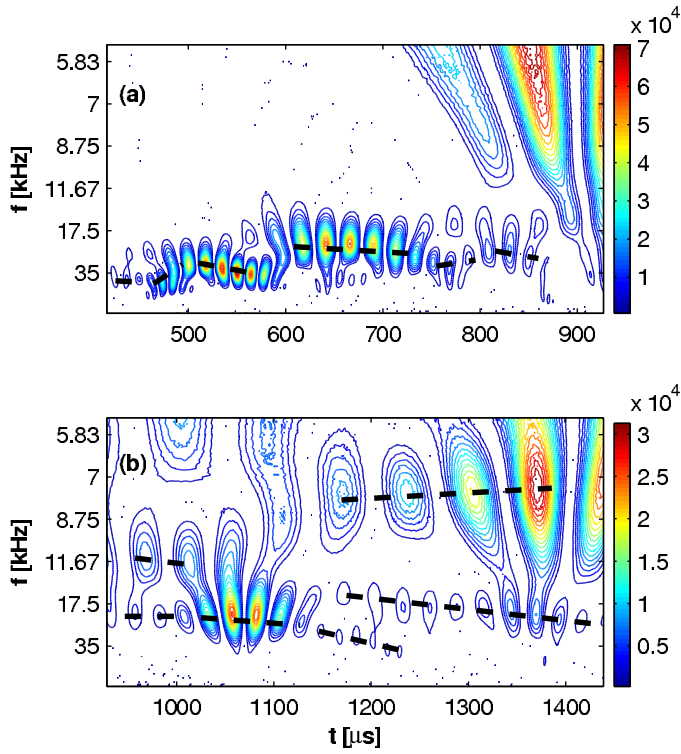


FIG. 4: (*color online*) Estimated CWT power spectrum of 512 data pts (a) before pt. B, (b) after pt. B. *Black dashed lines* show the horizontal ridges connecting maxima values in contour plot

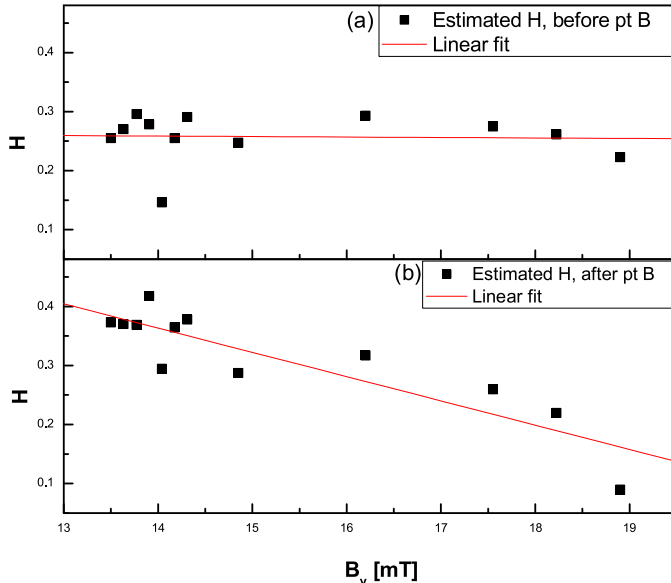


FIG. 5: (*color online*) Estimated (a) Hurst Exponent ( $H$ ) (a) before pt. B and (b) after pt. B for the various discharges of  $B_v$ , with each dataset of 512 pts, appended to result in 8192 pts

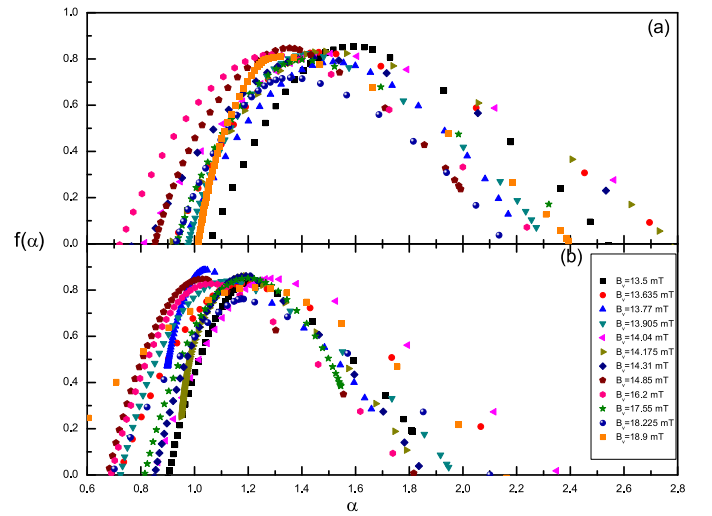


FIG. 6: (*color online*) Estimated multifractal singularity spectrum of 512 data pts before and after pt. B for the various discharges of  $B_v$ , with (a) before pt. B, (b) after pt. B

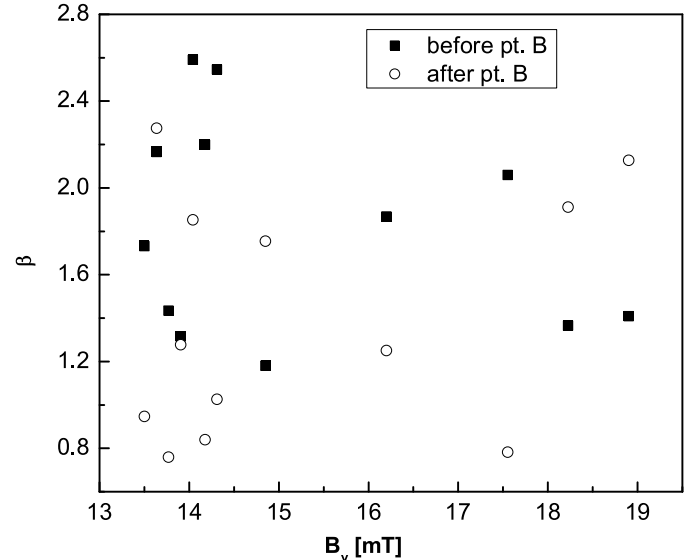


FIG. 7: Estimated degree of multifractality ( $\beta$ ) of 512 data pts before [*black, solid square*] and after pt. B [*orange, open circle*] for the various discharges of  $B_v$

power spectrum of the edge fluctuations show power law behavior ( $f^{-0.7}$ ) during extended phase [Fig. 3]. This indicates the possibility of the presence of multiscaling properties [13] in the electrostatic fluctuations. However before pt B we observed two sets of power law [Fig. 3].

The contour plot of the power spectrum obtained from the wavelet analysis depicted in Fig. 4, shows that before pt B, the power is observed to be concentrated at a particular frequency at each instant of time. Initially, till about  $550 \mu s$ , one finds the power to be concentrated at around  $35 kHz$  after which the  $17 kHz$  mode is seen to dominate. However for the signal after pt. B, the power

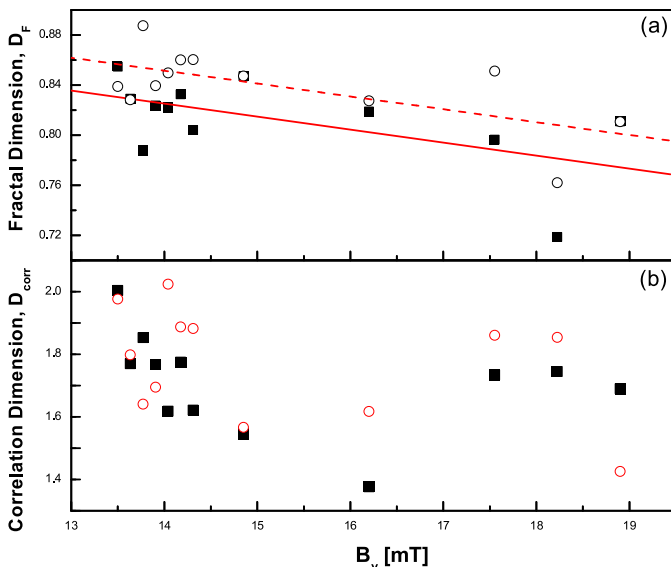


FIG. 8: (*color online*) Estimated (a) fractal dimension ( $D_F$ ) and (b) correlation dimension ( $D_c$ ) of 512 data pts before [black, solid square] and after pt. B [orange, open circle] for the various discharges of  $B_v$ , with (a) before pt. B, (b) after pt. B

is concentrated in two or three modes simultaneously at any given instant of time. The range, within which these dominant frequencies are observed is, 5 kHz to 35 kHz. The horizontal ridges connecting the maximum values show that the system is weakly chaotic as suggested by Chandre *et. al.* [20].

Hurst exponent (H) can also be used to determine the presence of stochasticity in the system. H is estimated using the Re-Scaled (R/S) Range analysis technique [14].  $H = 0.5$  implies a completely random/stochastic process.  $H < 0.5$  indicates long range antipersistence and  $H > 0.5$  implies long-range correlations. The plot of the Hurst exponent for the two regimes on either side of B plotted as a function of  $B_v$  is shown in Fig. 5. The Hurst exponent before pt. B is observed to be almost constant around 0.25 for the different  $B_v$  discharges, indicative of long range anti-correlations. However, after pt. B, we find that the extended discharge shows a tendency to have an  $H = 0.4 - 0.45$  at lower  $B_v$ . This again suggests that the extension in discharge duration seems to have a correlation to stochastic behaviour of the edge plasma fluctuations.

### A. Singularity spectrum from WTMM

The general method of measuring the singularity spectrum is by the box counting method [21]. But in order to get a more accurate result, it is better to use the multi-resolution analysis approach which can be obtained using the Wavelet Transform [22, 23, 24, 25, 26, 27]. This method of computing the singularity spectrum [23] of a

fractal signal consists of taking advantage of the time-scale partitioning of the WT given by the maxima representation of the WTMM method [28] to define a partition function which scales, in the limit  $a \rightarrow 0$ , in the following way:

$$Z(a, q) = \sum_{\{t_i(a)\}_i} |W_\Psi(a, t_i(a))|^q \sim a^{\tau(q)} \quad (1)$$

where,  $W_\Psi(a, t_i(a))$  is the wavelet coefficient and  $q$  is the moment considered.

At a given scale  $a$ , by not summing over the whole set of wavelet coefficients but only over the WTMM pts  $\{t_i(a)\}_i$ , one directly incorporates the multiplicative structure of the singularity distribution into the calculation of the partition function. Moreover one gets rid of the divergences for negative values. Thus a plot of  $\tau(q)$  vs  $q$  should ideally give an idea of the presence of monofractal or multifractals in the signal.

The singularity spectrum  $[f(\alpha) - \alpha]$  can subsequently be estimated by computing the Legendre Transform of  $\ln(Z(a, q))/\ln(a)$ . An alternative method is to define  $f(\alpha)$  by the canonical method defined as [23]:

$$\alpha(q) = \lim_{a \rightarrow 0} \frac{1}{\ln a} \sum_{\{t_i(a)\}_i} \hat{W}_\Psi(q; a, t_i(a)) \times \ln |W_\Psi(a, t_i(a))| \quad (2)$$

$$f(\alpha(q)) = \lim_{a \rightarrow 0} \frac{1}{\ln a} \sum_{\{t_i(a)\}_i} \hat{W}_\Psi(q; a, t_i(a)) \times \ln |\hat{W}_\Psi(q; a, t_i(a))| \quad (3)$$

where,

$$\hat{W}_\Psi(q; a, t_i(a)) = \frac{|W_\Psi(a, t_i(a))|^q}{\sum_{\{t_i(a)\}_i} |W_\Psi(a, t_i(a))|^q} \quad (4)$$

Thus one can directly obtain the set of singularity strengths ( $\alpha$ ) and the corresponding  $f(\alpha)$  spectrum from the log-log plots of equations (2 & 3). Subsequently, one can obtain the various dimensions from the relation  $(q - 1)D_q = q\alpha - f(\alpha)$  [29]. The maximum of this curve gives us the fractal dimension ( $D_0 = f(\alpha(q = 0)) = -\tau(0) \equiv D_F$ ) of the set of singularities of the signal. The right hand side of the spectrum corresponds to the negative  $q$ -moments and the left side the spectrum the positive  $q$ -moments. This latter mentioned method has been used in determining the multifractal spectrum in this paper. The analyzing wavelet used is the 9<sup>th</sup> derivative of the gaussian distribution.

The singularity spectrum before and after pt B, for the various discharges of  $B_v$  scan are presented in Fig. 6. We find that the multifractal spectrum is more asymmetric for the datasets, before pt. B whereas it tends to become more symmetric after pt. B.

The singularity spectrum basically gives an idea of the symmetry in generation of convergent and divergent singularities. Symmetry gives one an indication of multiplicative process sustaining a particular phenomenon [30]. Thus one can state that the fluctuations in the extended phase has its roots associated to some avalanche phenomena.

## V. DISCUSSIONS

The edge electrostatic fluctuation signals of discharges in the S.I.N.P tokamak, exhibiting an extension in the discharge duration after a fall from the peak current, has been analyzed in this paper. The analysis has been carried out from the point of view of applying nonlinear techniques and looking at the variation of these results with  $B_v$ . A comparison has also been made on either side of the transition point (B) of the discharge extension, within a given discharge.

The power law behaviour in the FFT spectrum of the electrostatic edge probe fluctuations indicates some sort of multicascading behaviour in the system. The wavelet spectrum also showed presence of chaotic behavior during the current extension phase. Hence, the singularity spectrum of the datasets were estimated, from which we estimated the degree of multifractality ( $\beta$ ), multifractal parameter ( $\lambda_M^2$ ), fractal dimension ( $D_F$ ) and correlation dimension ( $D_{corr}$ ). For the extended discharge regime, i.e. after pt. B, for the low  $B_v$  case, we found  $\beta \sim 0.6 - 1.2$ .  $D_F$  was of the order of  $0.88 - 0.84$  at lower  $B_v$  and decreasing further with increasing  $B_v$ .  $D_{corr}$  was of the order of  $1.6 - 2$  and  $\lambda_M^2 \sim 0.0008 - 0.003$ . The Hurst exponent (H) is observed to tend towards 0.5, during the extended phase (i.e. after pt. B). The largest Lyapunov exponents ( $\lambda_L$ ) were also found to be positive in these extended regimes. The estimates of  $\beta$ ,  $H$  and  $\lambda_L$  in the current extension phase indicates that the edge fluctuations exhibit a stochastic behaviour. The estimated correlation dimension from the Grassberger-Procaccia algorithm and from the singularity spectrum also indicates that the system's ergodicity increases in the extended phase of the discharge. Surrogate analysis test confirms that the source of these observations are from some inherent nonlinear phenomena.

The observations of the enhance energy levels in the HX bursts in the extended phase could be a result of better confinement of the high energy particles. Subsequently, onset of some instability could trigger the deconfinement of the particles, which are thereafter lost, through some stochastic process at the edge.

To cross-check whether the discharge could sustain any such beam-plasma interactions, we considered the condi-

tions that need to be satisfied given as [40]

$$\omega_{ce} > \omega_{pe} \quad (5)$$

$$v_{beam} > 3v_{cr} \left( \frac{\omega_{ce}}{\omega_{pe}} \right) \quad (6)$$

$$\nu_{eff} > \nu_e \quad (7)$$

where,  $\omega_{ce}$ ,  $\omega_{pe}$ ,  $v_{beam}$  and  $v_{cr}$  are the electron cyclotron frequency, electron plasma frequency, beam velocity and the critical velocity respectively.  $\nu_e$  is the electron collision frequency and  $\nu_{eff}$  is the effective collision frequency and is given by:

$$\nu_{eff} = \sqrt{\pi} \omega_{pe} \left( \frac{\omega_{pe}}{\omega_{ce}} \right) \epsilon^{-3/2} \lambda_r \quad (8)$$

$\lambda_r$  being the primary runaway flux generation factor and  $\epsilon = E_0/E_{cr}$ ,  $E_{cr}$  being the critical electric field for runaway generation and  $E_0 = V_{loop}/2\pi R_0$ .  $V_{loop}$  is the loop voltage. Using experimental results we find that in the extended discharge  $\omega_{ce} \approx 140.5$  GHz and  $\omega_{pe} \leq 100$  GHz which implies that condition 5 is satisfied. In order to evaluate the inequality of condition 6, we estimated the right hand side, denoting it as  $v_{beam}^{crit} (3v_{cr}[\omega_{ce}/\omega_{pe}])$ . We find  $v_{beam}^{crit}$  to be around  $3 \times 10^7$  m/s before pt B. This corresponds to a beam energy of 2keV. This is the minimum energy required for participation in a beam plasma instability. After pt B one finds an increase in  $v_{beam}^{crit}$  and it is of the order of  $10^8$  m/s (corresponding beam energy is 30 keV). Thus in the current extension phase the more energetic electrons will only satisfy condition 6. Subsequently to evaluate condition 7 we estimated  $\nu_e = 300$  kHz; for a 1 MeV beam, whereas  $\nu_{eff} = 1.2$  MHz during the current extension phase. However, for short discharges we did not find condition 7 to be satisfied, even though the other two were satisfied, towards the end of the discharge. Hence it could imply that the loss of runaway electrons observed in the extended phase could be a result of the participation of the higher energetic electrons in beam-plasma instabilities within the plasma column. The edge stochastic behaviour possibly helps in the ejection of these runaway electrons.

One still needs to look into other edge fluctuation behaviour, such as the magnetic, density and temperature fluctuations, in order to understand the role of the stochastic behaviour with the discharge extension. Such applications of nonlinear techniques to study the stochastic behavior could be an important method of research in future fusion devices. We intend to perform further experiments to study these phenomena in greater detail.

## ACKNOWLEDGEMENTS

We would like to thank the Prof. B. Sinha, Director, SINP for his support in carrying out this work. We also thank members of Plasma Physics Division, SINP for their help in carrying out the experiments presented

in this paper. One of the authors (RN) would like to acknowledge useful discussions on multifractal analysis with Prof. V.P. Budaev and Prof. M. Rajkovic. RN would also like to acknowledge Prof. K.H. Finken and organizers of SFP-2007 for providing financial support to attend and present this work in the Stochasticity in Fusion Plasmas-2007 Workshop, Julich Germany. An-

other coauthor (MN) also acknowledges discussions with Prof. J. C. Sprott on nonlinear analysis techniques.

## REFERENCES

- 
- [1] Ding Weixing, Huang Wie, Wang Xiaodong and C. X. Yu 1993 *Phys. Rev. Lett.* **70** 170
- [2] W. X. Ding, H. Q. She, W. Huang and C. X. Yu 1994 *Phys. Rev. Lett.* **72** 96
- [3] M. A. Hassouba, H.I. Al-Naggar, N.M. Al-Naggar and C. Wilke 2006 *Phys. Plasmas* **13** 073504
- [4] R. Jha, P.K. Kaw, S.K. Mattoo, C.V.S. Rao, Y.C. Saxena and Aditya Team 1992 *Phys. Rev. Lett.* **69** 1375
- [5] Md. Nurujjaman and A.N. Sekar Iyengar 2006 *Pramana J. Phys.* **67** 299, arXiv:physics/0611131 v1 14 Nov 2006
- [6] W. Engelhardt and W. Fenberg 1978 *Journal of Nuclear Materials* **76** & **77** 518
- [7] J.S.E. Portela, R.L. Viana and I.L. Caldas 2003 *Physica A* **317** 411
- [8] A. Samain, A. Grosman, T. Blenski, G. Fuchs and B. Steffen 1984 *Journal of Nuclear Materials* **128** & **129** 395
- [9] M. Lehnen *et. al.* 2005 *Journal of Nuclear Materials* **337-339** 171
- [10] E. Strumberger 1999 *Journal of Nuclear Materials* **266-269** 1207
- [11] H Renner, J Boscary, H Greuner, H Grote, F W Hoffmann, J Kisslinger, E Strumberger and B Mendelevitch 2002 *Nucl. Fus.* **44** 1005
- [12] T.E. Evans *et. al.* 2005 *Journal of Nuclear Materials* **337-339** 691
- [13] Md. Nurujjaman, and A.N.Sekar Iyengar 2007 *Phys Letts A* **360**, 717
- [14] B. A. Carreras *et al* 1999 *Phys. of Plasmas* **6** 1885
- [15] Grassberger P. and Procaccia I 1983 *Phys. Rev. Lett.* **50** 346
- [16] Grassberger P. and Procaccia I 1983 *Phys. Rev. A* **28** 2591
- [17] T. Schreiber 1999 *Phys. Reports* **308** 1-64
- [18] A. Wolf, J.B. Swift, H.L. Swinney and J.A. Vastano 1985 *Physica D* **16** 285
- [19] Ramesh Narayanan and A.N. Sekar Iyengar, *Rev. Sci. Instrum.* **77**, 033503 (2006)
- [20] C. Chandre, S. Wiggins, T. Uzer 2003 *Physica D* **181** 171
- [21] A.B. Chhabra, C. Meneveau, R.V. Jensen and K.R. Sreenivasan 1989 *Physical Review A* **40** 5284
- [22] J.F. Muzy, E. Bacry and A. Arneodo 1993 *Physical Review E* **47** 875
- [23] J.F. Muzy, E. Bacry and A. Arneodo 1991 *Phys. Rev. Lett.* **67** 3515
- [24] T.C. Halsey, M.H. Jensen, L.P. Kadanoff, I. Procaccia and B.I. Shraiman 1986 *Physical Review A* **33** 1141
- [25] B. Ph. Van Milligen, E. Sanchez, T. Estrada, C. Hidalgo, B. Branäs and B. Caueras 1995 *Physics of Plasmas* **2** 3017
- [26] M.V.A.P. Heller, Z.A. Brasillio, I.L. Caldas, J. Stockel and J. Petrzilka 1999 *Phys. of Plasmas* **6** 846 & *ICPP & 25th EPS Conf. on Controlled Fusion and Plasma Physics', Praha* (June 29- July 3, 1998) [1998 *ECA* **22C** 718]
- [27] S. Santoso, E.J. Powers, R.D. Bengston and A. Ouroua 1997 *Rev. Sci. Instr.* **68** 898
- [28] E. Bacry, J.F. Muzy and A. Arneodo 1993 *J. Stat. Phys.* **70** 635
- [29] P.E. Bak, N. Asakura, Y. Miura, T. Nakano and R. Yoshino 2001 *Phys. of Plasmas* **8** 1248
- [30] G.Y. Antar, P. Devynck, X. Garbet and S.C. Luckhardt 2001 *Phys. of Plasmas* **8** 1612
- [31] A. L. Bertozzi and A. V. Chhabra *Phys. Rev. E* 1994 **49** 4716
- [32] A. Silchenko and C-K Hu 2001 *Phys. Rev. E* **63** 041105
- [33] V. Budaev, Y. Kikuchi, Y. Uesugi and S. Takamura 2004 *Nucl. Fus.* **44** S108
- [34] Md. Nurujjaman, Ramesh Narayanan and A.N.Sekar Iyengar 2007 *Lect. Notes Phys.* **705** 499-505
- [35] Holger Kantz and Thomas Schreiber 2004 *Nonlinear Time Series Analysis* (Cambridge University Press; 2nd edition)
- [36] J. C. Sprott 2004 *Chaos and Time-Series Analysis* (Oxford University Press)
- [37] Guy Dori, Shmuel Fishman and S. A. Ben-Haim 2000 *Chaos* **10** 257
- [38] James Theiler, Stephen Eubank, André Longtin, Bryan Galdrikian and Dooyne Farmer 1992 *Physica D* **58** 77
- [39] T. Nakamura, and M. Small 2006 *International Journal of Bifurcations and Chaos* **16** in press
- [40] V.V. Plyusnin, 2002 *29th EPS Conference on Plasma Phys. and Contr. Fusion Montreux, 17-21 June 2002* **ECA-26B** P-4.097

